



ORIGINAL ARTICLE

# Assessment of buildings non-deterministic dynamic structural response when subjected to wind actions

*Avaliação da resposta estrutural dinâmica não-determinística de edifícios quando submetidos a ações do vento*

Leonardo Ferreira de Miranda<sup>a</sup> José Guilherme Santos da Silva<sup>a</sup>

<sup>a</sup>Universidade do Estado do Rio de Janeiro – UERJ, Faculdade de Engenharia – FEN, Programa de Pós-graduação em Engenharia Civil – PGECIV, Rio de Janeiro, RJ, Brasil

Received 04 April 2023

Revised 31 July 2023

Accepted 27 August 2023

Corrected 27 March 2024

**Abstract:** The construction of high-rise buildings has emerged as a constructive trend worldwide, and excessive vibration problems due to wind actions are becoming increasingly frequent. The Brazilian design standard NBR 6123 recommends that the transfer of wind actions used for structural analysis be carried out based on the pressure coefficients along the building facades for static analyses and considers their non-deterministic dynamic behaviour through a stochastic modelling method of the wind velocity field. To present an alternative approach to this methodology, this study aims to investigate the non-deterministic dynamic structural response of a real reinforced concrete building, considering the soil-structure interaction effect, using the pressure coefficients obtained through different methodologies such as numerical simulations using Computational Fluid Dynamics (CFD), international databases, and the recommendations of the Brazilian standard NBR 6123.

**Keywords:** high-rise buildings, dynamic structural analysis, human comfort assessment, computational fluid dynamics, numerical simulation.

**Resumo:** A construção de edifícios altos tem se mostrado uma tendência construtiva ao redor do mundo, e vibrações excessivas oriundas das ações do vento tem se tornado cada vez mais frequentes. A norma brasileira de projeto NBR 6123 recomenda que a transferência das ações de vento utilizadas para análise estrutural seja realizada com base nos coeficientes de pressão ao longo das fachadas do edifício, para análises estáticas, e considera o seu comportamento dinâmico não determinístico através de um método de modelagem estocástica do campo de velocidade do vento. Objetivando apresentar uma abordagem alternativa para esta metodologia, este estudo tem como objetivo investigar a resposta estrutural dinâmica não determinística de um edifício real de concreto armado, considerando o efeito da interação solo-estrutura, utilizando coeficientes de pressão obtidos por intermédio de metodologias distintas, tais como: simulações numéricas utilizando CFD (Computational Fluid Dynamics), bases de dados internacionais, e utilizando as recomendações da norma brasileira NBR 6123.

**Palavras-chave:** edifícios altos, análise estrutural dinâmica, avaliação do conforto humano, fluidodinâmica computacional, simulação numérica.

**How to cite:** L. F. Miranda and J. G. S. Silva, “Assessment of buildings non-deterministic dynamic structural response when subjected to wind actions,” *Rev. IBRACON Estrut. Mater.*, vol. 17, no. 4, e17407, 2024, <https://doi.org/10.1590/S1983-41952024000400007>

## 1 INTRODUCTION

The construction of high-rise buildings has become a constructive trend worldwide due to several factors, such as population growth, the urbanisation of large centres, reducing the usable areas for construction, the technological

**Corresponding author:** José Guilherme Santos da Silva. E-mail: [jgss@uerj.br](mailto:jgss@uerj.br)

**Financial support:** None.

**Conflict of interest:** Nothing to declare.

**Data Availability:** The data that support the findings of this research work are available from the corresponding author, J.G. Santos da Silva, upon reasonable request. This document has an erratum: <https://doi.org/10.1590/S1983-41952024000400011>



This is an Open Access article distributed under the terms of the Creative Commons Attribution License, which permits unrestricted use, distribution, and reproduction in any medium, provided the original work is properly cited.

development of construction materials and calculation methods in recent years, enabling the construction of buildings with increasingly slender elements, based on innovative and bold architectural projects. Because of these developments, structural problems due to excessive vibrations are becoming more frequent [1]–[3], as well as human discomfort caused by various dynamic actions, among which, the wind actions stand out as one of the most important [1], [3], [4].

The building design projects currently being carried out in Brazil are based on the recommendations of the Brazilian standard NBR 6123 [5] to consider the effect of wind on structures. In the NBR 6123 [5] formulation, the wind action is transmitted based on equivalent pressure coefficients applied along the building façades for static analyses, and considers the non-deterministic dynamic behaviour through a stochastic modelling method of the wind velocity field.

To present an alternative approach, this research work aims to investigate the non-deterministic dynamic structural behaviour of high-rise buildings and the assessment of human comfort, taking into account the wind pressure coefficients on the building façades calculated based on the use of different strategies. Initially, the analysis considers the wind pressure coefficients of the Brazilian standard NBR 6123 recommendations [5], which is characterised by the application of a single pressure coefficient along the building façade.

After that, the investigation considers the traditional database-assisted methods using data obtained in experimental tests in wind tunnels based on standardized geometries. In this context, the aerodynamic database created by the Tokyo Polytechnic University (TPU-AD) [6] and the Data-Enabled Design Module for High-Rise Buildings (DEDM-HR) [7] developed by Notre Dame University are powerful tools to provide the results of experimental tests in wind tunnels when studying wind loads on buildings.

Finally, the CFD (Computational Fluid Dynamics) numerical simulation, which nowadays plays an increasingly important role in high-rise building projects and is used as a sophisticated analysis method to predict the air flow on the structural system of the building, is studied and explored based on the use of the ANSYS Fluent software [8].

Since conducting experimental tests in wind tunnels is very expensive, much attention has been focused to this method, and intensive studies have been carried out, since an appropriate turbulence model in computational fluid dynamics (CFD) is still a challenge. Liu and Niu [9] compared the performance of different turbulence models in an analysis of the wind flow around an isolated building and found that the results for the average velocity on the windward façade of the building were consistent with the results of analyses in wind tunnels. On the other façades of the building, however, some turbulence models show better results than others.

Another very relevant issue is the correct representation of the boundary conditions of the fluid domain and the adequate representation of the wind velocity profile acting on the structure, which must be compatible with the chosen turbulence model. The refinement of the mesh is also of interest, since to represent the turbulence behaviour of the wind around the structure, a refinement of the entire flow domain is required, making the analyses involve a large number of elements and thus quite computationally onerous [10].

The research work is conducted based on a 40-storey reinforced concrete building that considers the soil-structure interaction effect. The model represents a real high-rise building located at the city of Balneário Camboriú, Brazil. The investigated building has a height of 140 m and floor dimensions of 10.44 m by 29.81 m. The building numerical model was developed to obtain a more realistic representation of the structural system, based on the Finite Element Method (FEM), using the ANSYS programme [11].

It must be emphasised that the results obtained in this work, using the wind pressure coefficients determined with the database-assisted methods [6], [7], the CFD simulations [8] and the Brazilian design standard NBR 6123 [5], revealed important quantitative differences reflecting on the dynamic structural response and the human comfort assessment. Also, as it will be shown, the flexible direction of the studied building model is an issue of concern since the displacements and accelerations values have exceeded the serviceability limits in several design situations.

## 2 INVESTIGATED STRUCTURAL MODEL

In this investigation, a real 40-storey building with a height of 140 m and floor dimensions of 10.44 m by 29.81 m was investigated considering the soil-structure interaction effect [2]. The building structural system consists of concrete beams, columns, and slabs. The bases of the columns are connected to a raft foundation, which serves as a pile cap for the foundation piles. The 3D view and a detail of the foundation system are shown in Figure 1, and the geometric characteristics of the building can be seen in Figure 2.

The building is made of reinforced concrete elements and presents a modulus of elasticity equal to 32 GPa ( $E = 32 \text{ GPa}$ ), Poisson's ratio of 0.2 ( $\nu = 0.2$ ), specific weight equal to  $25 \text{ kN/m}^3$  ( $\rho = 25 \text{ kN/m}^3$ ) and damping ratio of 0.02 ( $\xi = 2\%$  [5]). On the other hand, the aerodynamic damping effect [12] was not considered, due to the high computational cost and the minimum impact on the results [13]. It is worth highlighting that the building structural model attends all requirements related to the ultimate and serviceability limit states recommended by the Brazilian design standard NBR 6118 [14].

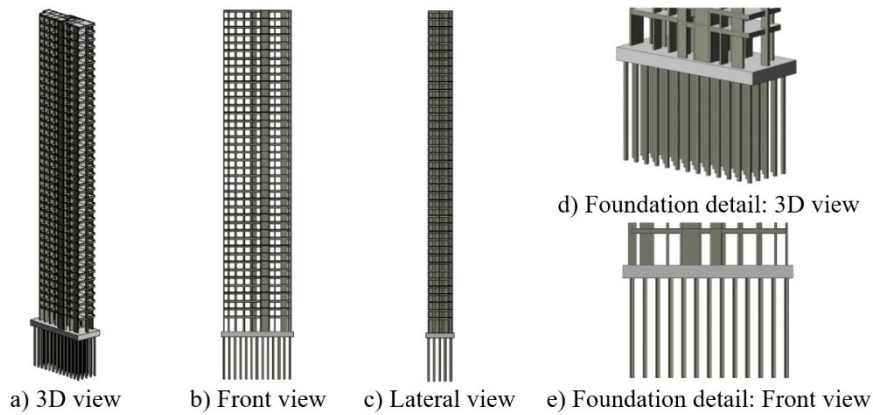


Figure 1. Investigated reinforced concrete building and foundation views

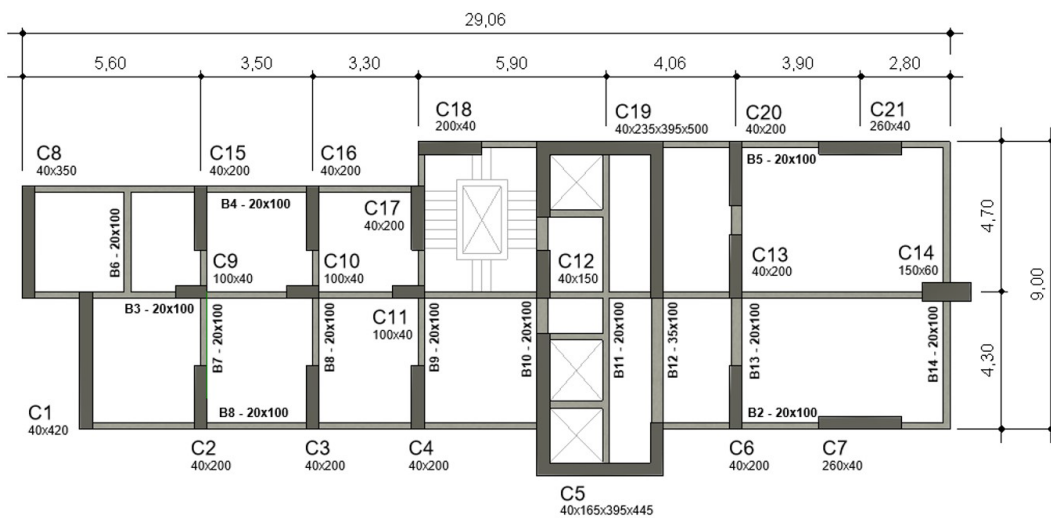


Figure 2. Floor plan of the reinforced concrete building model

### 3 FINITE ELEMENT MODELLING OF THE BUILDING

The numerical model developed for the building non-deterministic dynamic structural analyses utilises the usual mesh refinement techniques present in numerical simulations based on the use of the Finite Element Method (FEM) through the ANSYS software [11]. The investigated building finite element model is illustrated in Figure 3.

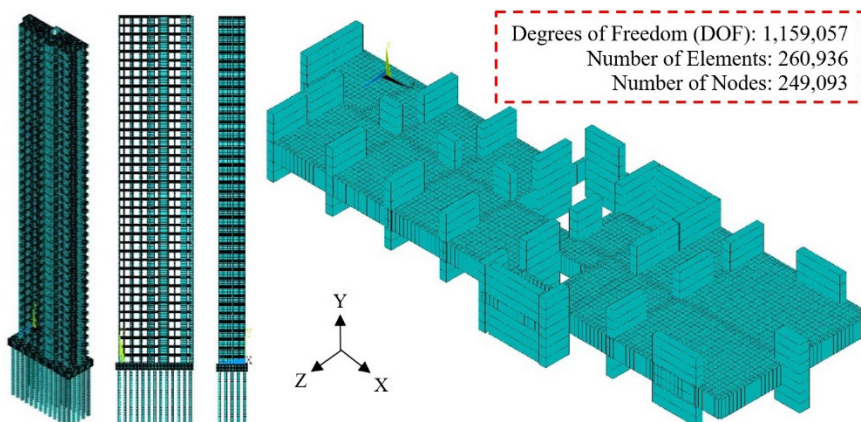


Figure 3. Building finite element model

Regarding the finite element model, the reinforced concrete beams and columns were represented by three-dimensional BEAM44 finite elements, which consider bending and torsion effects. On the other hand, the concrete slabs were simulated using SHELL63 finite elements. Considering the foundation elements, the foundation slab was represented by a solid element (SOLID45) and the piles were also represented by BEAM44 elements. In the developed building finite element mesh, the finite elements of the slabs, beams and raft foundation present size of 25 cm, while the columns and pile elements present 50 cm and 100 cm of size, respectively. It must be emphasized that the numerical model was subjected to several convergence tests to determine an appropriate level of refinement aiming at a good representation of the building dynamic response. The structural elements were connected by rigid connections.

As for the boundary conditions, the pile bases only restrict the vertical and horizontal translational displacements, while the rotational movements are free. In addition, to represent a more realistic behaviour of the building foundation, horizontal spring elements (COMBIN14) were placed along the pile heights. Finally, it should be mentioned that in this study it was assumed that the concrete presents a linear-elastic and isotropic behaviour.

#### 4 MODAL ANALYSIS: EIGENVALUES AND EIGENVECTORS

The investigated natural frequencies (eigenvalues) and vibration modes (eigenvectors) of the reinforced concrete building were determined based on numerical extraction methods (modal analysis) considering a free vibration analysis through the ANSYS programme [11]. Figure 4 shows the natural frequencies and vibration modes of the building model.

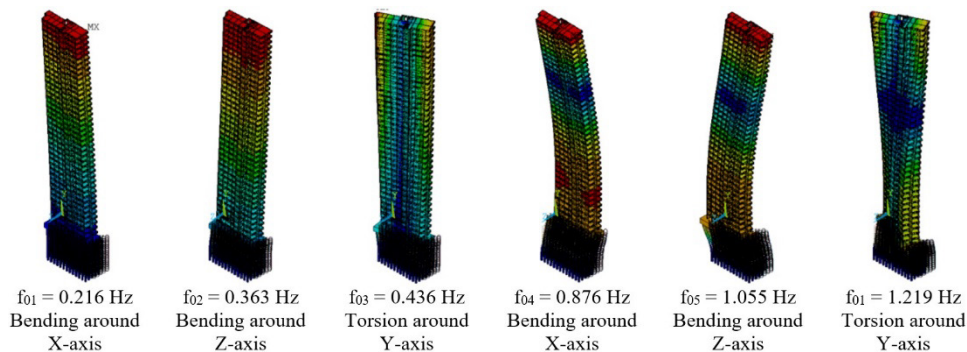


Figure 4. Natural frequencies and vibration modes of the building model

The analysis results show that the building presents a very pronounced bending effect around the X-axis (Z-direction). The structure fundamental frequency is equal to 0.216 Hz, which makes it very flexible. According to the Brazilian standard NBR 6123 [5], buildings with fundamental period higher than 1 second (fundamental frequency less than 1 Hz) can have a strong fluctuating behaviour in the mean wind direction. Moreover, as will be seen in section 7, this frequency lies in the high energy transfer zone of the Kaimal power density spectrum, maximising the effects of wind loads acting on the building façades. Having in mind the other natural frequencies and vibration modes, it can be seen that these magnitudes are relevant up to the fourth vibration mode, with the Z-direction having special importance due to its high flexibility.

#### 5 DETERMINATION OF THE PRESSURE COEFFICIENTS

To obtain the building non-deterministic dynamic structural response, a process must be followed, which is divided into four methods and three steps. In this study, the Brazilian standard NBR 6123 [5] recommendations (Method I) and the CFD simulation [8] (Method II) were used only in the first step, associated to the wind pressure coefficients calculations. After that, the non-deterministic dynamic wind loads acting on the building façades are determined (Step 2), based on the Spectral Representation Method (SRM).

The aerodynamic database developed by the Tokyo Polytechnic University [6] (Method III) already provides the non-deterministic dynamic wind loads (Step 2), which are calculated based on pressure monitors attached to the building model in the wind tunnel tests. Based on these non-deterministic loads, a transient analysis can be performed (Step 3) to determine the building displacements and accelerations. On the other hand, the Data-Enabled Design Module for High-rise Buildings [7] (Method IV) already provides directly the displacements and accelerations (Step 3). Figure 5 shows a flowchart summarising the developed analysis methodology. After that, aiming to investigate the building non-deterministic dynamic structural response and assess the human comfort, the results are compared with recommended limits described in technical standards and research papers.

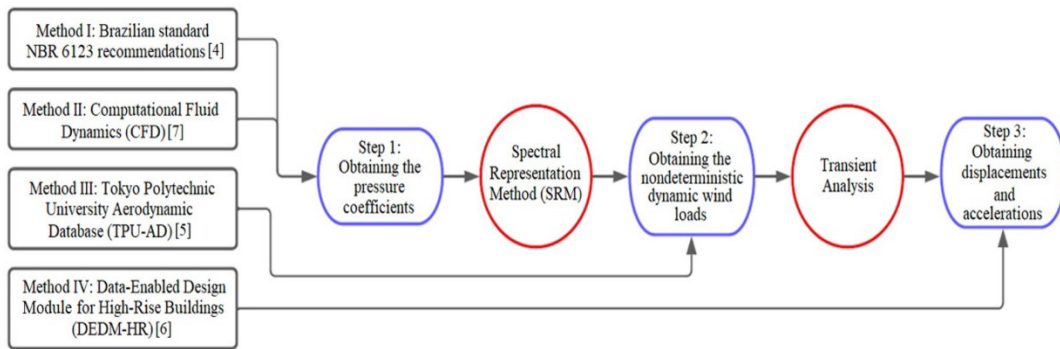


Figure 5. Flowchart of the developed analysis methodology

### 5.1 Brazilian standard NBR 6123 recommendations [5]

The recommendations of the Brazilian standard NBR 6123 [5] aim to establish the conditions for determining the static and dynamic forces due to wind actions on the building façades, based on the use of a characteristic wind velocity represented by Equation 1, where  $V_0$  is the basic wind velocity in m/s,  $S_1$  is a topographical factor,  $S_3$  is the probability factor and  $S_2$  is the factor that takes into account the roughness of the terrain, the dimensions of the structure and the height above the terrain, represented by Equation 2, where  $F_r$  is the gust factor,  $b$  is a meteorological parameter,  $p$  is the exponent of the potential law and  $Z$  is the height in metres. Table 1 show the parameters used in this study, that result in a wind velocity of 31.6 m/s at the building top. Figure 6 shows the velocity profile defined by these parameters. It must be emphasized that the wind velocity (Figure 6) only represents the static part of the wind. However, the wind also has a fluctuating part, which is determined by the developed analysis methodology presented in section 7.

$$\bar{V}(z) = V_0 S_1 S_2 S_3 \tag{1}$$

$$S_2 = b F_r \left(\frac{z}{10}\right)^p \tag{2}$$

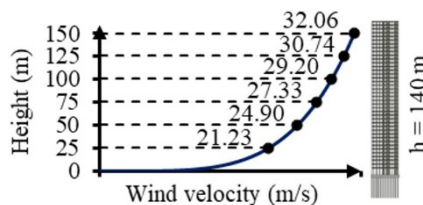


Figure 6. Velocity profile: Brazilian standard NBR 6123 [5]

Table 1. Parameters adopted in the Brazilian standard NBR 6123 [5] method

Type	Value	Description
Basic wind velocity	45 m/s	Isopleths: Balneário Camboriú/SC
Ground Class	IV	Urban Region
$S_1$ factor	C	Dimension higher than 50 m
$S_3$ factor	1.00	Flat ground
$F_r$ factor	0.78	63% for 10 years
$b$ parameter	0.69	Gust factor
$p$ parameter	0.71	Meteorological parameter
Analysis period	0.23	The exponent of the potential law
	600 s	Standard time interval

### 5.2 Computational Fluid Dynamics (CFD) numerical simulation [8]

The governing equations that model incompressible, transient, and isothermal flows are the Navier-Stokes equations. They describe the three-dimensional motion of viscous fluid substances by applying a time-dependent continuity equation for mass conservation [Equation 3] and a time-dependent momentum conservation equation [Equation 4], where  $\rho$  is the density of the fluid in  $\text{kg/m}^3$ ,  $\partial \vec{v} / \partial t$  represents the change of velocity with time in  $\text{m/s}^2$ ,  $(\nabla \cdot \vec{v}) \vec{v}$  represents the velocity

in the direction of the fluid flow in m/s,  $\rho \vec{g}$  are external forces such as gravity, given in N,  $\nabla p$  is the pressure gradient, given in Pa, and  $\mu \cdot \nabla^2 \vec{v}$  is related to the internal stresses due to viscous effects, given in Pa.

$$\nabla \cdot \vec{v} = 0 \quad (3)$$

$$\rho \cdot \left( \frac{\partial \vec{v}}{\partial t} + (\vec{v} \cdot \nabla) \vec{v} \right) = \rho \vec{g} - \nabla p + \mu \cdot \nabla^2 \vec{v} \quad (4)$$

Nevertheless, there is still no proof that there are always solutions for three-dimensional motion, or if there are, that they do not contain a singularity. In practice, the Navier-Stokes equations are quite good for solving simple problems such as laminar flows in a steady state, where the flow has high viscosity and low velocity. However, according to Asyikin [15], most flows are turbulent and can be described as chaotic, fluctuating and random flows. These random fluctuations in the flow are also carriers of important quantities such as force and energy. Turbulent flows are highly unstable, three-dimensional and a time-dependent process. In this flow regime, viscosity begins to take on a random character. For this reason, it is necessary to develop ways to predict this behaviour so that the terms of the equations involving the viscosity are complete. Therefore, these solutions must be determined based on CFD (Computational Fluid Dynamics) simulations.

In this direction, there is a need to choose a turbulence model suitable for the problem. According to Wilcox et al. [16], there are several turbulence models in the literature. One model included in the ANSYS Fluent programme [8] is the Standard k- $\epsilon$  model proposed by Launder and Spalding [17]. This model applies to fully developed turbulent flows [18], gives satisfactory results and is the most used. Moreover, it requires little simulation effort compared to other turbulence models and is relatively accurate [17]–[20].

### 5.2.1 Turbulence model

The k- $\epsilon$  turbulence model is one of the models known as two-equation models [21], where the velocity and length scales are obtained by solving two transport equations. The variable k stands for the turbulent kinetic energy and  $\epsilon$  is the dissipation rate, where the transport equations are given by Equations 5 and 6, respectively.

$$\frac{\partial k}{\partial t} + \frac{\partial k v_i}{\partial x_i} = \frac{\partial}{\partial x_j} \left[ \left( \mu + \frac{\mu_t}{\sigma_k} \right) \frac{\partial k}{\partial x_j} \right] + P - \epsilon \quad (5)$$

$$\frac{\partial \epsilon}{\partial t} + \frac{\partial \epsilon v_i}{\partial x_i} = \frac{\partial}{\partial x_j} \left[ \left( \mu + \frac{\mu_t}{\sigma_\epsilon} \right) \frac{\partial \epsilon}{\partial x_j} \right] + C_{1\epsilon} P - C_{2\epsilon} \frac{\epsilon^2}{k} \quad (6)$$

In Equations 5 and 6,  $\sigma_k$  and  $\sigma_\epsilon$  are the inverse effective Prandtl number, P is the term used to generate the mean turbulent kinetic energy, and  $C_{1\epsilon}$  and  $C_{2\epsilon}$  are empirical constants. The turbulent viscosity  $\mu_t$  is given by Equation 7, where  $C_\mu$  is also an empirical constant. It must be emphasised that the constants from Equations 5 to 7 come from the correlation of experimental data from different turbulent flows [22] and are as follows:  $C_\mu = 0.09$ ,  $C_{1\epsilon} = 1.44$ ,  $C_{2\epsilon} = 1.92$ ,  $\sigma_k = 1.0$  and  $\sigma_\epsilon = 1.3$ .

$$\mu_t = \rho C_\mu \frac{k^2}{\epsilon} \quad (7)$$

This model is widely used in fluid motion simulations, and its popularity is explained by its robustness, economy, and reasonable accuracy for a wide range of turbulent fluid motion problems. However, this model also has its limitations and as its strengths and weaknesses became known, improvements were made to the model to improve its performance. Considering these improvements, variants of this model have been developed and some of these variants are available in the ANSYS Fluent programme [8], such as the RNG k- $\epsilon$  model, which is used as the turbulence model for performing the CFD simulations of this research work. The RNG k- $\epsilon$  model was derived using a rigorous statistical technique called Reorganization Group Theory (RNG). It is similar in form to the Standard k- $\epsilon$  model but contains refinements that make it more accurate and reliable than the Standard k- $\epsilon$  model for a larger class of flows. For more details, see the ANSYS Fluent User Guide [8].

### 5.2.2 Wind velocity profile

The input conditions for a horizontally homogeneous atmospheric boundary layer can be derived analytically by solving the turbulence model and the equations of the wall functions for equilibrium. Richards and Hoxey [23] derived the velocity profile by a logarithmic equation [Equation 8], and the corresponding k and  $\epsilon$  profiles [Equations 9 and 10], where  $\kappa = 0.4$  and  $C_\mu = 0.085$ .

$$\bar{V}(z) = \frac{u_*}{\kappa} \ln\left(\frac{z+z_0}{z_0}\right) \tag{8}$$

$$k = \frac{u_*^2}{\sqrt{c_\mu}} \tag{9}$$

$$\epsilon = \frac{u_*^3}{\kappa(z+z_0)} \tag{10}$$

In this research work, the friction velocity  $u_*$  in the atmospheric boundary layer is equal to 2.98 m/s, and the roughness length  $z_0$  is 2 m, which corresponds to a well-developed urban area where tall buildings are typically located [24]. These parameters result in a wind velocity of 31.7 m/s at the building top. The velocity profile can be seen in Figure 7. As this is a steady-state analysis, it must be emphasized that the wind profile presented in Figure 7 only represents the static part of the wind. The fluctuating part of the wind is determined based on the analysis methodology presented in section 7.

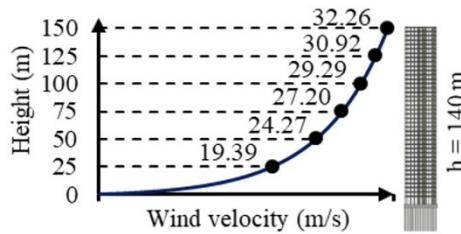


Figure 7. Velocity profile: CFD numerical simulation [8]

### 5.2.3 CFD modelling

The mathematical modelling begins defining the boundaries of the fluid domain, which play an important role in the CFD modelling. According to Abu-Zidan et al. [10], the boundaries are mostly non-physical, so their influences on the flow domain are a source of error in the simulation. Therefore, the boundaries should be placed far away from the building to avoid significant influences on the results. However, if the boundaries are placed too far away, the calculation costs of the model could increase. The fluid domain has an inlet side, where the velocity profile is inserted and an outlet side, where the flow is assumed to be fully developed and the static pressure is zero. The lateral and upper boundaries were walls where the shear stresses of the fluid were not considered, and the lower boundary was considered to be a wall with a roughness length of two metres (see Figure 8).

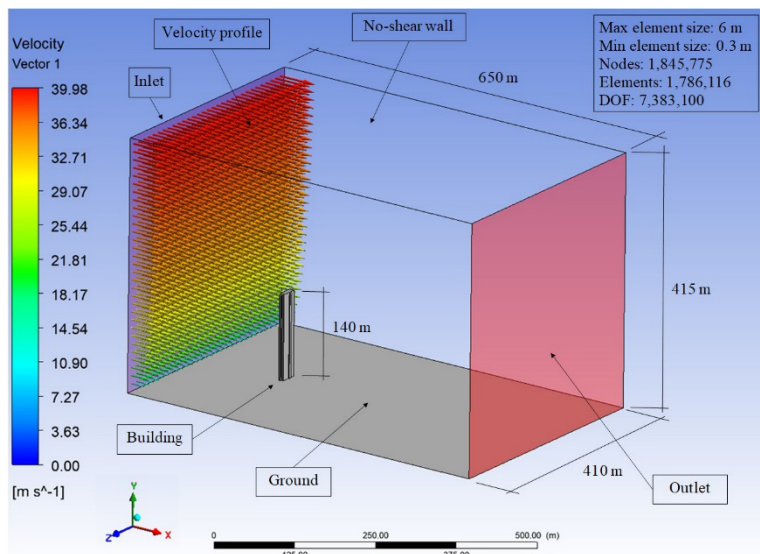


Figure 8. Boundary conditions of the fluid domain

Another potential source of error in this study lies in the spatial discretisation. The impact of this error is mitigated by maintaining a consistent meshing configuration for all simulation cases in this study. This prevents deviations in the results caused

by abrupt variations in the mesh [25]. To maintain a consistent mesh near the building, the larger domain grids are created by extruding the boundary cells from smaller domains. Therefore, the MultiZone method was employed to generate a structured mesh of hexahedral elements with a growth rate of 1.05 and a target skewness below 0.5, as illustrated in Figure 9. Despite the wind being sensitive to changes in the architecture of the building [26], to utilise this method, small simplifications of curved regions from the original architectural model were considered, resulting in minimal impact on the results.

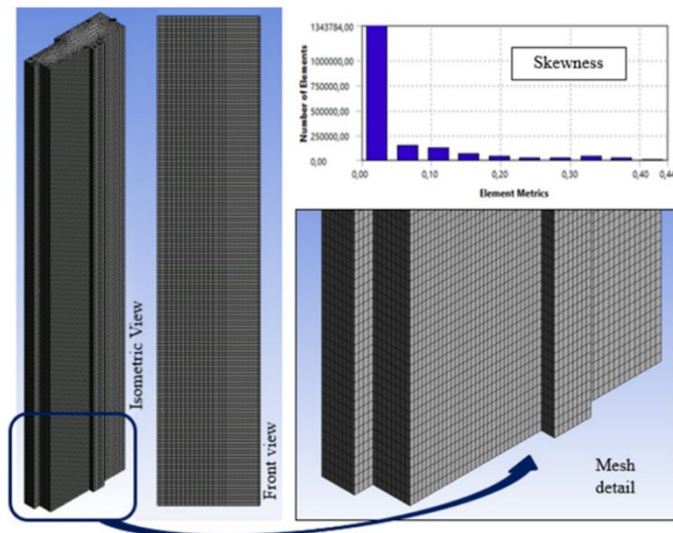


Figure 9. Reinforced concrete building mesh details

As for the solver settings, pseudo-transient analyses were performed using the pressure-velocity coupling solution method with coupled scheme. The spatial discretisation for the gradient was the Green-Gauss node-based and second-order equations were used for the pressure, momentum, turbulent kinetic energy, and turbulent dissipation rate.

Once all the appropriate parameters were set, it is time to insert the velocity profile. Since it follows the form of a logarithmic equation, it cannot be inserted directly but has to be inserted via User Defined Function (UDF) instead. Finally, to measure the wind pressure, several pressure monitors were attached to the building façades. Figure 10 shows the pressure monitors placed on the investigated building model. Along the numerical analyses, some pressure monitors were selected to monitor the wind pressure behaviour during the substeps of the analyses in order to assess whether convergence was achieved.

Regarding the wind direction, due to the asymmetry of the building, four CFD analyses were carried out, considering the wind acting in the directions of Z(+), Z(-), X(+) and X(-) (see Figure 11). In sequence, Figure 12 shows the pressure contour plot and the wind velocity contour plot for the studied building, when the wind blows in the direction of Z(+).

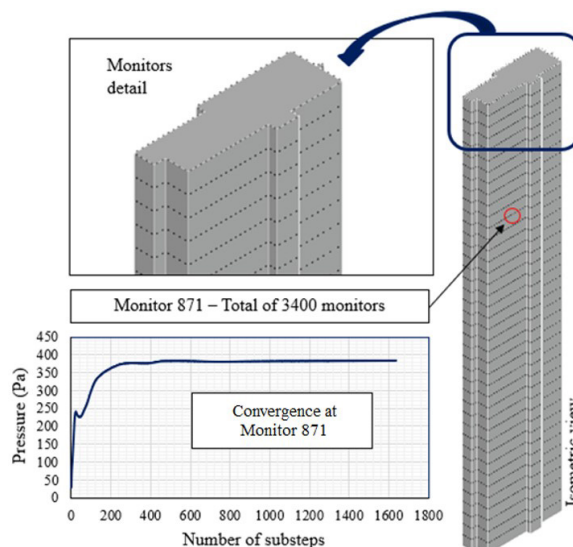


Figure 10. Pressure monitors placed on the building model

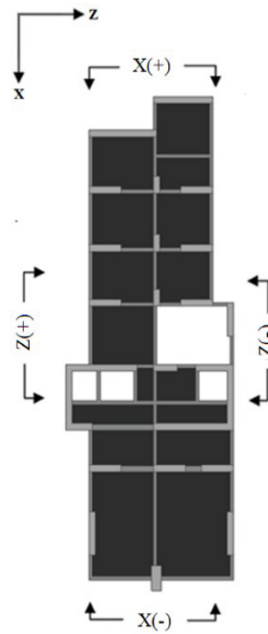


Figure 11. Wind orientations

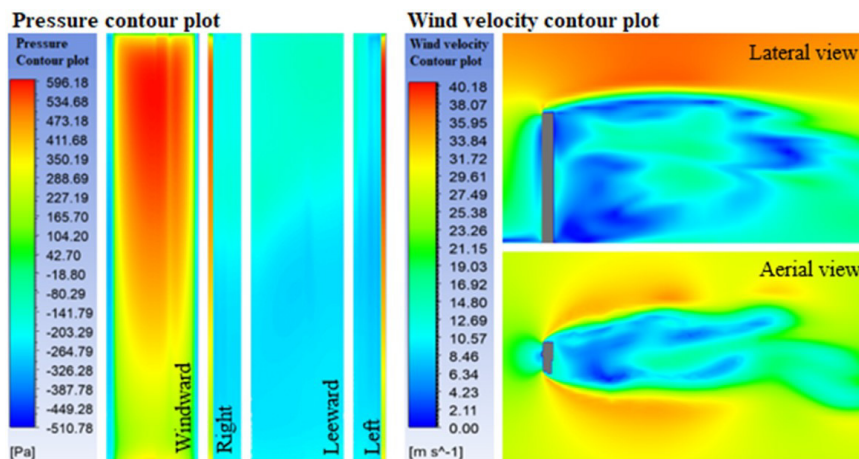


Figure 12. Contour plots: real investigated building model [Z(+) direction]

### 5.3 The database-assisted methods

Considering the results quantitative comparisons related to the Brazilian standard NBR 6123 recommendations [5] and the CFD numerical simulations [8], this investigation also considers the traditional database-assisted methods based on the data obtained through experimental tests in wind tunnels associated to standardized geometries. In this context, the aerodynamic database developed by the Tokyo Polytechnic University (TPU-AD) [6] and the Data-Enabled Design Module of High-Rise Buildings (DEDM-HR) [7] developed by the Notre Dame University will be assessed. It must be emphasized that all details about the analysis methodology of these database-assisted methods are found in references [6], [7].

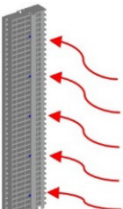
## 6 ASSESSMENT OF THE WIND PRESSURE COEFFICIENTS

After the wind pressure coefficients calculation on the building façades, it is important to compare these coefficients calculated by each assessed method. Therefore, the pressure coefficients of the windward, right, leeward, and left building façades are presented in Tables 2 to 5. The pressure coefficients were determined based on a wind reference velocity measured at the top of the building. It is worth to note that the platform DEDM-HR [7] (Method IV) does not

provide results for pressure coefficients. In this context, the pressure coefficients on the façades of the investigated building were determined using the recommendations of the Brazilian standard NBR 6123 [5] (Method I), the CFD simulations [8] (Method II), and the results provided by the Tokyo Polytechnic University Aerodynamic Database (TPU-AD [6] (Method III)). It must be emphasized that the TPU-AD [6] (Method III) results were considered as reference because the wind pressure coefficients are determined based on experimental tests in wind tunnels.

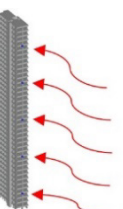
Based on the results presented in Tables 2 to 5, and having in mind that NBR 6123 [4] (Method I) recommends the use of an average wind pressure coefficient along the building façade, when comparing the results calculated through the three methods, NBR 6123 [5] (Method I), the CFD simulations [8] (Method II) and TPU-AD database [6] (Method III), the quantitative differences between the wind pressure coefficients can be quite significant. Looking at the results presented in Table 2 (windward façade), it can be observed that the TPU-AD [6] and CFD [8] methods presented very close wind pressure coefficients (maximum difference: 5.3%), while the NBR 6123 [5] method presents a compatible average value with the two methods. On the other hand, when analysing Table 4 (leeward façade), it can be verified that the TPU-AD [6] and NBR 6123 [5] methods presented close pressure coefficients (maximum difference: 17.6%), while the CFD [8] simulation presented lower values. Analysing the results presented in Tables 3 and 5 (right and left façades), it can be observed that the TPU-AD [6] and NBR 6123 [5] methods presented compatible results (maximum difference: 28.2%), while the CFD [8] method presented lower values. It must be emphasized that there was a reasonable difference in the wind pressure coefficients when the three methods were investigated. In general, it was concluded that the NBR 6123 [5] method, presented the highest values, and the CFD [8] simulation presented the lowest magnitudes.

**Table 2.** Wind pressure coefficients at windward façade



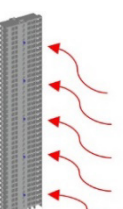
Pressure Coefficients	TPU-AD [6] (Method III)		CFD [8] (Method II)		NBR 6123 [5] (Method I)		DEDM-HR [7] (Method IV)	
	Value	%	Value	%	Value	%	Value	%
Position [h (m)]								
36 <sup>th</sup> floor: h = 126 m	0.93	100.0	0.96	103.2	0.80	86,0	-	-
28 <sup>th</sup> floor: h = 98 m	0.89	100.0	0.91	102.2	0.80	89,9	-	-
20 <sup>th</sup> floor: h = 70 m	0.75	100.0	0.79	105.3	0.80	106,7	-	-
12 <sup>th</sup> floor: h = 42 m	0.60	100.0	0.62	103.3	0.80	133.3	-	-
4 <sup>th</sup> floor: h = 14 m	0.40	100.0	0.41	102.5	0.80	200,0	-	-

**Table 3.** Pressure coefficients at right façade



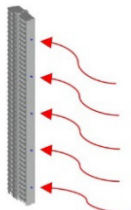
Pressure coefficients	TPU-AD [6]		CFD [8]		NBR 6123 [5]		DEDM-HR [7]	
	Value	%	Value	%	Value	%	Value	%
Position								
36 <sup>o</sup> floor: h = 126 m	-1.04	100.0	-0.31	29.8	-1.0	96.1	-	-
28 <sup>o</sup> floor: h = 98 m	-0.95	100.0	-0.30	31.6	-1.0	105.3	-	-
20 <sup>o</sup> floor: h = 70 m	-0.91	100.0	-0.37	40.6	-1.0	109.9	-	-
12 <sup>o</sup> floor: h = 42 m	-0.88	100.0	-0.45	51.1	-1.0	113.6	-	-
4 <sup>o</sup> floor: h = 14 m	-0.81	100.0	-0.42	51.8	-1.0	123.4	-	-

**Table 4.** Pressure coefficients at leeward façade



Pressure coefficients	TPU-AD [6]		CFD [8]		NBR 6123 [5]		DEDM-HR [7]	
	Value	%	Value	%	Value	%	Value	%
Position								
36 <sup>o</sup> floor: h = 126 m	-0.63	100	-0.22	34.9	-0.6	95.2	-	-
28 <sup>o</sup> floor: h = 98 m	-0.55	100	-0.27	49.1	-0.6	109.1	-	-
20 <sup>o</sup> floor: h = 70 m	-0.51	100	-0.43	84.3	-0.6	117.6	-	-
12 <sup>o</sup> floor: h = 42 m	-0.53	100	-0.43	81.1	-0.6	113.2	-	-
4 <sup>o</sup> floor: h = 14 m	-0.53	100	-0.41	77.3	-0.6	113.2	-	-

**Table 5.** Pressure coefficients at left façade



Position	TPU-AD [6]		CFD [8]		NBR 6123 [5]		DEDM-HR [7]	
	Value	%	Value	%	Value	%	Value	%
36° floor: h = 126 m	-1.01	100.0	-0.41	40.6	-1.0	99.0	-	-
28° floor: h = 98 m	-0.97	100.0	-0.44	45.4	-1.0	103.1	-	-
20° floor: h = 70 m	-0.96	100.0	-0.50	52.1	-1.0	104.2	-	-
12° floor: h = 42 m	-0.86	100.0	-0.47	54.6	-1.0	116.3	-	-
4° floor: h = 14 m	-0.78	100.0	-0.41	52.6	-1.0	128.2	-	-

### 7 MATHEMATICAL MODELLING OF THE WIND LOADS

As mentioned before, the wind presents a dynamic behaviour (static and fluctuating part) as shown in Equation 11, where  $V(z, t)$  is the non-deterministic wind velocity,  $\bar{V}(z)$  is the static part of the wind, and  $\hat{V}(z, t)$  is the fluctuating part of the wind, all given in m/s. The static part of the wind is calculated based on two of the methods proposed in chapter 5 - the Brazilian standard NBR 6123 recommendations [5] or the wind velocity profile proposed by Richards and Roxey [23] for the CFD simulation [8]. On the other hand, the fluctuating part of the wind has non-deterministic characteristics, and statistical parameters such as mean, standard deviation and spectral density function are used for its representation. Considering that the wind properties are unstable and random, a second-order non-deterministic ergodic process with stationary properties has been used for the mathematical modelling of the wind loads.

$$V(z, t) = \bar{V}(z) + \hat{V}(z, t) \tag{11}$$

Despite the uncertainties involved in attempting to represent the wind non-deterministic behaviour [27], signals with non-deterministic properties can be obtained, according to Shinozuka and Jan [28], by the Spectral Representation Method (SRM), which uses the spectral density function of the signal to calculate the amplitudes and frequencies of each harmonic. In this study, the SRM was applied to generate the wind fluctuating part, as shown in Equation 12, where  $f$  represents the frequency,  $S^v(f)$  refers to the increment of the wind power spectral density,  $f_i$  is the frequency with respect to the harmonic  $i$ ,  $\Delta f$  is the frequency increment, and  $\theta_i$  is the random phase angle uniformly distributed in the interval  $[0-2\pi]$ .

$$\hat{V}(z, t) = \sum_{i=1}^N \sqrt{2S^v(f_i)\Delta f} \cos(2\pi f_i t + \theta_i) \tag{12}$$

The fluctuating part of the wind velocity  $\hat{V}(t)$  is generated with random phase angles, and the amplitude of each harmonic is calculated based on the spectral density determined using the Kaimal spectrum [Equation 13], where  $fS(f)$  corresponds to the spectral density associated with the longitudinal component of the turbulence with frequency  $f$ . The term  $X$  is the dimensionless frequency and can be represented by Equation 14, and the term  $u_*$  is the friction velocity, represented by Equation 15, where  $\bar{V}(Z)$  is the static part of the wind velocity at height  $Z$ , and  $K$  is the Karman constant.

$$\frac{fS(f,Z)}{u_*^2} = \frac{200X}{(1+50X)^{5/3}} \tag{13}$$

$$X(f, Z) = \frac{fZ}{\bar{V}(Z)} \tag{14}$$

$$u_* = \frac{K\bar{V}(Z)}{\ln\left(\frac{Z}{Z_0}\right)} \tag{15}$$

It should be emphasised that, according to the Kaimal power density spectrum, the building fundamental frequency determined by the modal analysis (see section 4) is in the range of higher energy transfer peaks associated with low natural frequencies (see Figure 13). Therefore, a dynamic structural analysis (forced vibration) is required to evaluate the building serviceability limit states.

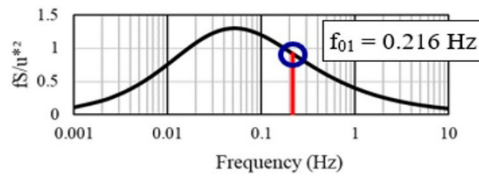


Figure 13. Kaimal power density spectrum

Subsequently, the non-deterministic wind-induced response of the building can be calculated by summing the static and fluctuating parts (random vibration) of the wind. Finally, the dynamic forces acting on the building façades are calculated at several different points of the structure using Equation 16, where  $\rho$  is the air density ( $\rho = 1,225 \text{ kg/m}^3$ ),  $V_i(z, t)$  is the non-deterministic wind velocity, in m/s, acting on the façade of the building,  $C_p$  is the respective pressure coefficient and  $A_i$  is the respective area of influence in  $\text{m}^2$ . The extended mathematical formulation of the wind force is shown in Equation 17. Thus, according to the developed mathematical formulation, 30 series of non-deterministic wind loads were generated considering the pressure coefficients determined by the Brazilian standard NBR 6123 [5] and the CFD numerical simulations [8]. The non-deterministic wind loads series were generated considering an interval of 600 seconds (10 minutes).

$$F(z, t) = \frac{1}{2} \rho V_i(z, t)^2 A_i C_p \tag{16}$$

$$F(z, t) = 0,613 C_p A \left[ \bar{V}(z) + \sum_{i=1}^n \sqrt{2S^v(f_i)\Delta f} \cos(2\pi f_i t + \theta_i) \right]^2 \tag{17}$$

This way, Figures 14 and 15 show, respectively, a typical example of the non-deterministic wind load in the time and frequency domains acting on a specific section of the building windward façade. The building fundamental frequency ( $f_{01} = 0.216 \text{ Hz}$ ) is in resonance with an excitation frequency of relatively high amplitude, indicating that the wind dynamic load is amplified at this frequency. Considering the building 6<sup>th</sup> natural frequency ( $f_{06} = 1.219 \text{ Hz}$ ), this eigenvalue is in resonance with a wind load frequency of much lower amplitude, meaning that the excitation is not amplified at this frequency, see Figure 15. It should be mentioned that the NBR 6118 [14] requires that accidental loads must be multiplied by a coefficient  $\psi_1$  of 0.3 in serviceability verifications.

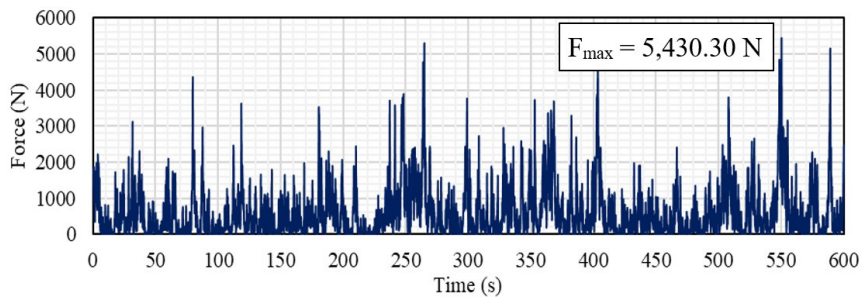


Figure 14. Dynamic wind loads in the time domain calculated through the SRM

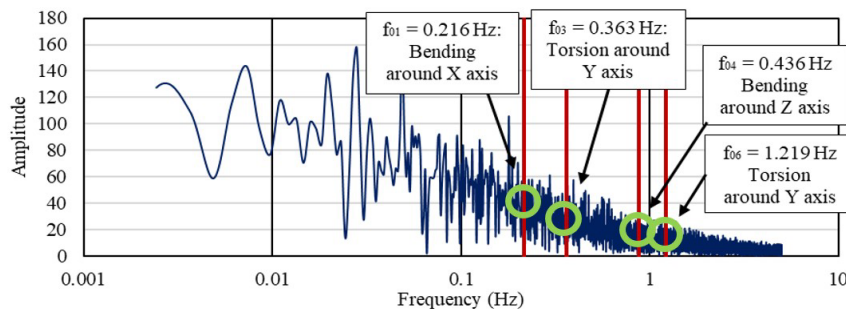


Figure 15. Dynamic wind loads in the frequency domain calculated through the SRM

## 8 ANALYSES RESULTS AND DISCUSSIONS

To investigate the non-deterministic dynamic structural behaviour and assess human comfort of the studied reinforced concrete building, the results quantitative analysis is performed based on the recommended limits for displacements and accelerations.

### 8.1 Displacements and accelerations limit values: serviceability limit state

Regarding the limits for displacements in the serviceability limit state, the Brazilian design standard NBR 6118 [14] prescribes that the maximum displacement at the top of the building must not exceed the limit value  $H/1700$ , where  $H$  is the building total height. When the accelerations are considered, the perception limits have been set by technical standards and research papers on the perception thresholds of the population worldwide, defining the criteria as limits that can be exceeded in a certain return period. In Brazil, the Brazilian standard NBR 6123 [5] recommends that, for the human comfort assessment, the maximum amplitude must not exceed  $0.1 \text{ m/s}^2$ , and it is considered permissible that the maximum acceleration can be exceeded once every 10 years. The same return period exists in North America, where the typical practise is to use 10-15 milli-g for peak horizontal accelerations at the top floor for residential buildings [29]. However, in regions with frequent typhoons and hurricanes, a shorter return period, e.g. one year, may be required.

Kareem et al. [30] have summarised some of the perception criteria currently in use (see Figure 16). Among these, the RMS acceleration limit of 8 to 10 milli-g for 10 years of recurrence interval proposed by Kareem [31] is included. The Japanese standard AIJ [32] is also present, which defines different levels of peak acceleration perception, with H2 typically used for residential applications. Based on the results of several studies, Melbourne and Palmer [33] also proposed limits of peak acceleration (represented by the light blue line in Figure 16) considering different return periods. Reed [34] defined a constant perception limit of 5 milli-g for a return period of six years. Irwin [35] proposed an RMS acceleration curve represented by the yellow line, and the same RMS acceleration is proposed by the ISO 6897 [36]. In the same direction, Goto [37] established that a limit value of  $0.8 \text{ m/s}^2$  must be considered to avoid situations of extreme discomfort. On the other hand, Bachmann et al. [38] proposed different tolerance levels to people subjected to vibration effects based on peak acceleration values, varying from imperceptible to intolerable levels.

### 8.2 Analyses results: quantitative and qualitative assessments

Since the non-deterministic wind loads were determined, transient analyses were performed on the investigated building, and the displacements and accelerations were calculated in time domain. This way, Tables 6 and 7 show the results based on the use of the NBR 6123 [5] and CFD [8] methodologies in terms of peak and RMS accelerations, considering 30 wind loads non-deterministic series.

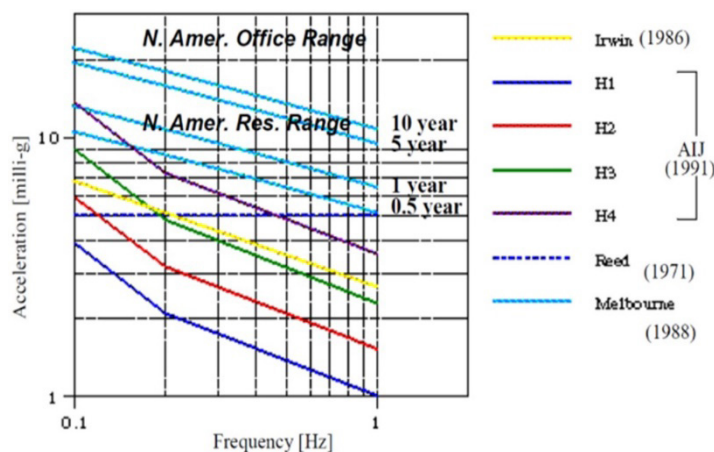


Figure 16. Perception criteria of acceleration limits in the serviceability limit state [30]

In addition, Figures 17 to 19 show the behaviour of the building displacement responses, in time and frequency domains for a wind incidence associated to the Z-direction, considering the dynamic structural analysis based on the

NBR 6123 [5], CFD [8] and TPU-AD [6] methodologies, respectively. As can be seen, the signal of the displacements in the time domain in the Z-direction presents very high amplitudes, showing that this is a very flexible direction, and vibration problems could be a topic of concern (see Figures 17 to 19). On the other hand, this is not true for the building displacement responses in the X-direction, where the amplitude is lower, indicating that this direction is stiffer and should not represent a problem (see Figures 17 to 19). The same qualitative and quantitative conclusions can be drawn from the analysis of the building acceleration responses, as presented in Tables 6 and 7 and illustrated in Figures 20 to 22.

When the building response in the frequency domain is investigated, it can be verified that the energy transfer peaks associated to the first four natural frequencies of the structure (see Figure 4) can be seen clearly, indicating that the forced vibration analyses using the non-deterministic time series provided compatible results (see Figures 17 to 22).

**Table 6.** CFD acceleration results [ $\text{m/s}^2$ ]

CFD [8] series	X direction		Z direction	
	Peak	RMS	Peak	RMS
1	0.037	0.010	0.115	0.034
2	0.040	0.011	0.127	0.035
3	0.036	0.011	0.134	0.032
4	0.044	0.011	0.101	0.033
5	0.044	0.010	0.144	0.037
6	0.036	0.010	0.133	0.033
7	0.044	0.011	0.151	0.036
8	0.029	0.010	0.122	0.035
9	0.032	0.010	0.101	0.034
10	0.031	0.011	0.126	0.033
11	0.041	0.011	0.127	0.037
12	0.030	0.009	0.141	0.037
13	0.036	0.010	0.134	0.038
14	0.039	0.010	0.141	0.036
15	0.036	0.011	0.166	0.036
16	0.038	0.010	0.135	0.038
17	0.040	0.011	0.128	0.035
18	0.046	0.011	0.135	0.031
19	0.033	0.011	0.115	0.035
20	0.038	0.010	0.094	0.030
21	0.036	0.010	0.128	0.034
22	0.036	0.010	0.111	0.034
23	0.037	0.011	0.115	0.031
24	0.036	0.011	0.129	0.035
25	0.034	0.010	0.119	0.030
26	0.030	0.010	0.141	0.034
27	0.050	0.011	0.104	0.032
28	0.034	0.010	0.126	0.037
29	0.048	0.011	0.149	0.034
30	0.034	0.009	0.113	0.033
Mean ( $\mu$ )	0.037	0.010	0.127	0.034
Standard Deviation ( $\sigma$ )	0.005	0.000	0.016	0.002
$\mu + 2\sigma$	0.048	0.011	0.159	0.039

**Table 7.** NBR 6123 acceleration results [m/s<sup>2</sup>]

NBR 6123 [5] series	X direction		Z direction	
	Peak	RMS	Peak	RMS
1	0.049	0.015	0.163	0.044
2	0.066	0.016	0.116	0.036
3	0.055	0.015	0.148	0.046
4	0.053	0.015	0.153	0.047
5	0.050	0.015	0.195	0.048
6	0.060	0.016	0.175	0.044
7	0.056	0.015	0.127	0.043
8	0.081	0.018	0.170	0.046
9	0.042	0.013	0.124	0.044
10	0.058	0.016	0.153	0.048
11	0.025	0.008	0.143	0.044
12	0.025	0.007	0.130	0.046
13	0.025	0.007	0.146	0.044
14	0.025	0.008	0.144	0.044
15	0.032	0.007	0.146	0.038
16	0.028	0.008	0.155	0.045
17	0.039	0.008	0.150	0.045
18	0.031	0.008	0.165	0.046
19	0.029	0.008	0.128	0.046
20	0.026	0.008	0.197	0.050
21	0.032	0.008	0.127	0.038
22	0.026	0.007	0.127	0.044
23	0.024	0.008	0.116	0.042
24	0.022	0.007	0.119	0.034
25	0.032	0.008	0.150	0.046
26	0.023	0.007	0.158	0.046
27	0.027	0.007	0.147	0.050
28	0.020	0.006	0.164	0.045
29	0.025	0.008	0.176	0.047
30	0.028	0.008	0.148	0.049
Mean ( $\mu$ )	0.037	0.010	0.149	0.044
Standard Deviation ( $\sigma$ )	0.016	0.004	0.021	0.004
$\mu + 2\sigma$	0.068	0.018	0.190	0.052

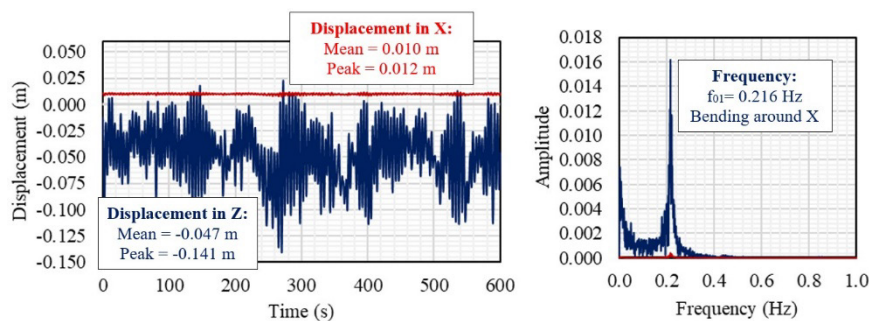


**Figure 17.** Displacement in the time and frequency domains: NBR 6123 [5] (Z-direction)

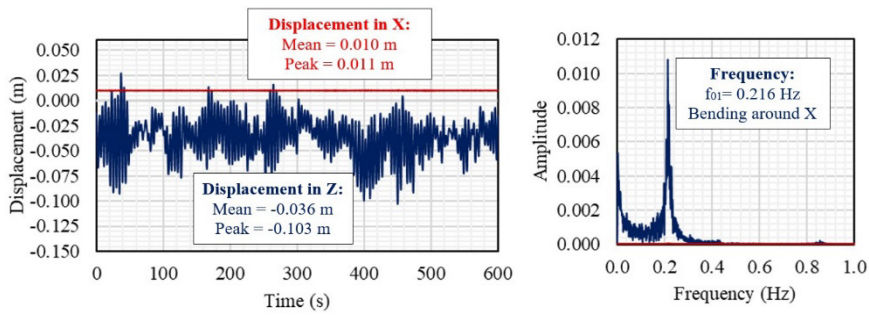


Figure 18. Displacement in the time and frequency domains: CFD [8] (Z-direction)

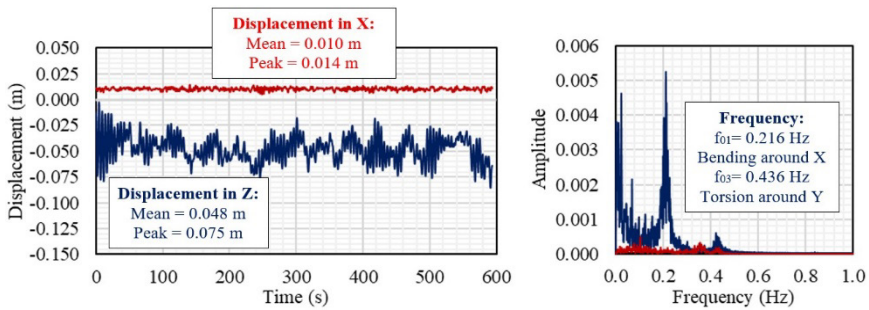


Figure 19. Displacement in the time and frequency domains: TPU-AD [6] (Z-direction)

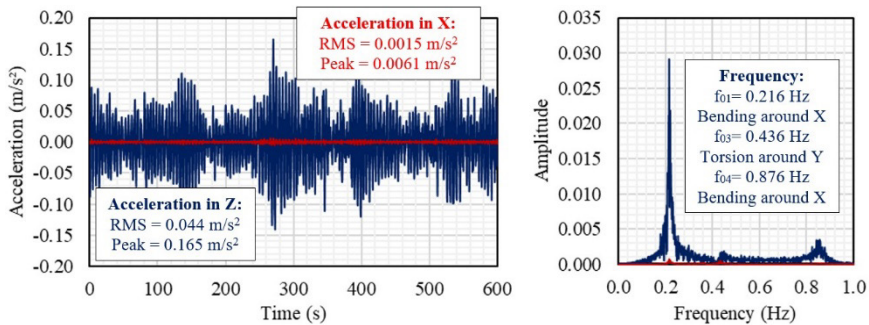


Figure 20. Acceleration in the time and frequency domains: NBR 6123 [5] (Z-direction)

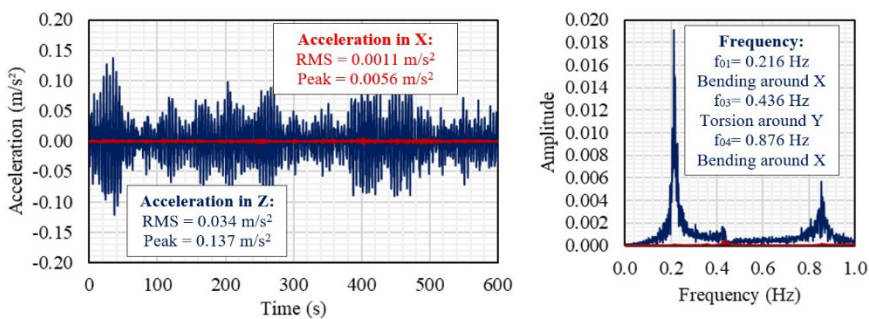


Figure 21. Acceleration in the time and frequency domains: CFD [8] (Z-direction)

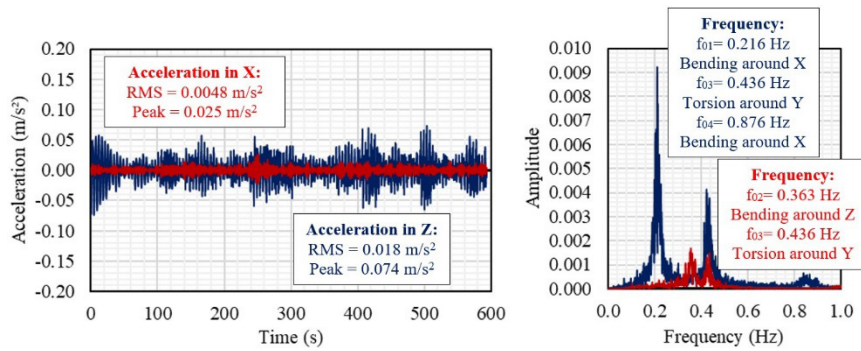


Figure 22. Acceleration in the time and frequency domains: TPU-AD [6] (Z-direction)

It must be emphasized that when analysing the X-direction results, the method TPU-AD [6] shows higher amplitudes of accelerations and displacements than the amplitudes obtained through the methods NBR 6123 [5] and CFD [8]. This fact possibly indicates that the TPU-AD methodology [6] can capture the wind vortex effects on the building façades, which have a significant influence on the displacements and accelerations perpendicular to the wind direction (although, due to the large difference in stiffness between the two directions, it is not possible to verify the actual impact of this effect on the results). This conclusion is supported by the analysis results in the frequency domain, where the energy transfer peaks related to the natural frequencies can be seen in the Z-direction (see Figures 17 to 22), but when the X-direction is investigated, only the TPU-AD [6] response, especially the accelerations, show these natural frequency peaks (see Figure 22). It must be emphasised that, in theory, the CFD simulation [8] should also be able to capture the wind vortex effect when a wind transient simulation is performed. However, a three-dimensional transient CFD simulation [8] requires very high computational effort. Therefore, a stationary CFD numerical simulation was performed in this research work.

Aiming to assess the serviceability limit state, the human comfort was evaluated based on the peak and RMS acceleration values calculated on the last building habitable floor and comparing these values to the acceleration limits (see section 8.1). This way, Table 8 and Figure 23 show the peak acceleration values of the building model obtained in the X and Z-directions using the four analysis methodologies investigated in this work, while Table 9 and Figure 24 show the corresponding RMS acceleration values. This way, four peak acceleration limits, for a return period of 10 years, were used to assess the peak accelerations: the limit proposed by the Brazilian standard NBR 6123 [5], proposed by Melbourne and Palmer [33], based on the Japanese standard AIJ [32], and the acceleration limit commonly used in North America, mentioned by Isyumov [29]. On the other hand, for the evaluation of the RMS accelerations, three limit values were used: the limit proposed by Kareem [31], by Irwin [35], and by the international technical standard ISO 6897 [36].

When analysing the X-direction (stiffer direction), it is noticeable that the accelerations are very far from the proposed limits for human comfort assessment, indicating that this direction does not represent a vibration problem (see Tables 6 to 9 and Figures 23 and 24). However, when analysing the Z-direction (flexible direction), although all the RMS acceleration values are within the recommended limits, the same cannot be said about the peak accelerations, since these limits were surpassed in almost all design situations (see Tables 6 to 9 and Figures 23 and 24). These results show the relevance of considering the wind non-deterministic dynamic behaviour on the buildings design.

Table 8. Peak accelerations [m/s<sup>2</sup>]

Method	Z-direction		X-direction	
	Value	%	Value	%
NBR 6123 [5]	0.149	100.0	0.037	100.0
CFD [8]	0.127	85.2	0.038	102.7
TPU-AD [6]	0.203	136.2	0.041	110.8
DEDM-HR [7]	0.177	118.8	0.059	159.4
Limit 1: NBR 6123 [5]	0.1	-	0.1	-
Limit 2: N. America [29]	0.147	-	0.147	-
Limit 3: Melbourne and Palmer [33]	0.106	-	0.104	-
Limit 4: AIJ [32]	0.081	-	0.064	-

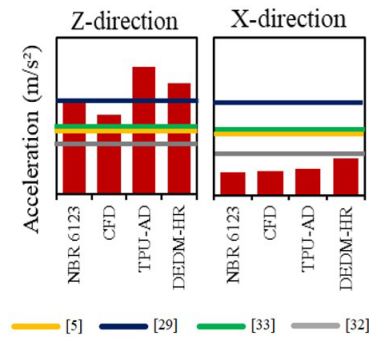


Figure 23. Peak accelerations

Table 9. RMS accelerations [m/s<sup>2</sup>]

Method	Z-direction		X-direction	
	Value	%	Value	%
NBR 6123 [5]	0.044	100.0	0.010	100.0
CFD [8]	0.034	77.3	0.010	100.0
TPU-AD [6]	0.042	95.4	0.008	80.0
DEDM-HR [7]	0.046	104.5	0.015	150.0
Limit 1: Kareem [31]	0.078	-	0.078	-
Limit 2: Irwin [35]	0.049	-	0.039	-
Limit 3: ISO 6897 [36]	0.049	-	0.039	-

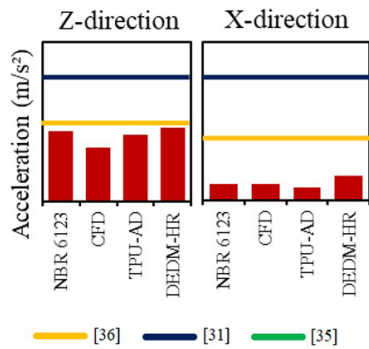


Figure 24. RMS accelerations

Considering the assessment of the peak displacement values at the top of the building, the displacement limit proposed by the NBR 6118 [14] was utilised. This way, Table 10 and Figure 25 present the peak displacement results at the building top in X and Z-directions. The results followed the same pattern presented when the peak acceleration results were investigated. The recommended limits were surpassed in almost all investigated project situations when the Z-direction was analysed (see Table 10 and Figure 25).

Table 10. Peak displacements [m]

Method	Z direction		X direction	
	Value	%	Value	%
NBR 6123 [5]	0.135	100.0	0.018	100.0
CFD [8]	0.103	76.3	0.018	100.0
TPU-AD [6]	0.085	64.0	0.019	105.5
DEDM-HR [7]	0.174	128.9	0.018	100.0
Limit: Kareem [31]	0.082	-	0.082	-

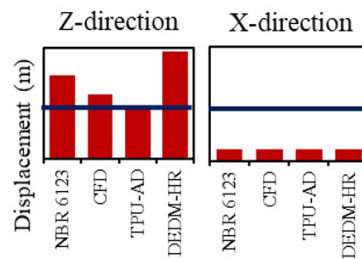


Figure 25. Peak displacements

It is important to analyse the results based on comparisons between the four methods (NBR 6123 [5]; CFD [8]; TPU-AD [6]; DEDM-HR [7]), considering qualitative and quantitative aspects. Based on a qualitative point of view, it can be observed that these methods are converging for the same conclusion: the investigated building has no excessive vibration problems in the X-direction but shows an intense oscillatory behaviour when the Z-direction is evaluated, surpassing the recommended design limits. This convergence indicates that the methodology consistently represents the building dynamic behaviour.

On the other hand, quantitative differences can be observed, when the four analysis methodologies were investigated. The peak acceleration results showed differences between 12.81% and up to 37.44% when the Z-direction was studied, while in the X-direction these differences vary from 2.63% to up to 37.29%. Regarding the RMS accelerations, there are differences between 4.35% and up to 26.09% in Z-direction, while these differences can reach 46.67% in X-direction. Finally, the displacements presented differences varying from 17.47% to up to 51.15%, in Z-direction, while the X-direction presented differences that can reach 5.26%, see Tables 6 to 10 and Figures 23 to 25.

## 9 CONCLUSIONS

In this investigation, the non-deterministic dynamic structural behaviour of a real high-rise reinforced concrete building was analysed, considering the wind pressure coefficients acting on the structure façades, based on the use of four methodologies: the Brazilian standard NBR 6123 recommendations [5], by using CFD simulations [8], and through the use of traditional database-assisted methods, such as the aerodynamic database developed by the Tokyo Polytechnic University (TPU-AD) [6] and the Data-Enabled Design Module for High-Rise Buildings (DEDM-HR) [7] developed by the University of Notre Dame. This way, the following conclusions can be drawn from the results presented in this work:

1. Based on the wind pressure coefficient values determined from the TPU-AD database [6], computational fluid dynamics (CFD) simulations [8], and in accordance with the recommendations of the Brazilian standard NBR 6123 [5], which indicates the use of an average wind pressure coefficient for each building facade, it can be concluded that the quantitative differences between the pressure coefficients can be quite significant: a) When the windward facade is considered, it can be verified that the TPU-AD [6] and CFD [8] methods presented very close wind pressure coefficients (maximum difference: 5.3%), while the NBR 6123 [5] method presents a compatible average value with the two methods; b) Analysing the leeward facade, it can be observed that the TPU-AD [6] and NBR 6123 [5] methods presented close pressure coefficients (maximum difference: 17.6%), while the CFD [8] simulation presented lower values; c) When the right and left façades were investigated, it can be observed that the TPU-AD [6] and NBR 6123 [5] methods presented compatible results (maximum difference: 28.2%), while the CFD [8] method presented lower values. This conclusion is quite relevant because these differences between the wind pressure coefficients calculated based on the use of different methodologies can affect the displacement and acceleration values, and the assessment of the building human comfort.

2. Analysing the acceleration and displacement results, in the time and frequency domains, it could be seen that only the TPU-AD [6] method was able to capture the effects of wind vortex acting on the building. However, because of the large difference in stiffness between the two investigated directions, it was not possible to verify the actual impact of this effect on the results. This way, it is therefore recommended to perform the same study on a building with the same geometry and stiffness in both directions.

3. When assessing the human comfort, the building presented structural responses within the design limits, when the X-direction was studied, indicating that this direction does not represent a vibration problem. In contrast, regarding the Z-direction, the peak acceleration values proved to be an issue of concern, exceeding these limits in almost all situations. The same pattern occurred when analysing the peak displacement results. Considering that this study was performed on a real structure, the results show the relevance of considering the wind non-deterministic dynamic behaviour on the design of high-rise buildings.

4. When comparing the four analysis methods, relevant quantitative differences can be seen. The peak acceleration values presented differences between 12.81% and up to 37.44% in the Z-direction, while these differences vary from 2.63% to up to 37.29% in the X-direction. Regarding the RMS accelerations, there are differences between 4.35% and up to 26.09% in the Z-direction, while the differences can reach 46.67% in the X-direction. The peak displacements presented differences varying from 17.5% to up to 51.15% in the Z-direction, while the X-direction presented differences up to 5.26%. These differences are relevant because they can modify the final building human comfort assessment.

## ACKNOWLEDGEMENTS

The authors gratefully acknowledge the financial support for this research work provided by the Brazilian Science Foundation's CNPq, CAPES and FAPERJ.

## REFERENCES

- [1] L. F. Miranda, "Study of the dynamic structural behaviour of high-rise buildings when subjected to non-deterministic wind actions considering pressure coefficients based on the use of different strategies," Ph.D. dissertation, Civ. Eng. Postgrad. Program., State Univ. Rio de Janeiro, Rio de Janeiro, 2023.
- [2] L. S. Bastos, "Study of buildings dynamic structural behaviour subjected to wind actions considering the soil-structure interaction effect," Ph.D. dissertation, Civ. Eng. Postgrad. Program., State Univ. Rio de Janeiro, Rio de Janeiro, 2019.
- [3] M. H. El Ouni, M. Abdeddaim, S. Elias, and N. B. Kahla, "Review of vibration control strategies of high-rise buildings," *Sensors*, vol. 22, no. 21, pp. 8581, 2022, <http://dx.doi.org/10.3390/s22218581>.
- [4] A. Barile, "Evaluation of buildings dynamic structural response when subjected to wind actions based on comparisons between different methods to calculate the peak accelerations," M.S. thesis, Civ. Eng. Postgrad. Program., State Univ. Rio de Janeiro, Rio de Janeiro, 2019.
- [5] Associação Brasileira de Normas Técnicas, *Forças Devidas ao Vento em Edificações*, ABNT NBR 6123, 1988.
- [6] The School of Architecture & Wind Engineering. Graduate School of Engineering. Tokyo Polytechnic University, "Aerodynamic database of high-rise buildings," in *Wind Eff. Build. Urban Environ.*, Tohyo, 2003.
- [7] D. K. Kwon and A. Kareem, "A multiple database-enabled design module with embedded features of international codes and standards," *Int. J. High-Rise Buildings*, vol. 2, no. 3, pp. 257–269, 2013.
- [8] Ansys, Inc., *Ansys® Fluent, Release 19.2, Help System, ANSYS Fluent User's Guide v19.2*, ANSYS, Inc., 2018.
- [9] J. Liu and J. Niu, "CFD simulation of the wind environment around an isolated high-rise building: an evaluation of SRANS, LES and DES models," *Build. Environ.*, vol. 96, pp. 91–106, 2016, <http://dx.doi.org/10.1016/j.buildenv.2015.11.007>.
- [10] Y. Abu-Zidan, P. Mendis, and T. Gunawardena, "Optimizing the computational domain size in CFD simulations of tall buildings," *Heliyon*, vol. 7, no. 4, e06723, 2021, <http://dx.doi.org/10.1016/j.heliyon.2021.e06723>.
- [11] Ansys, Inc., *Ansys® Mechanical APDL, Release 12.1, Help System, ANSYS Theory Reference v12.1*. Ansys, Inc., 2010.
- [12] H. Carvalho, G. Queiroz, P. M. L. Vilela, and R. H. Fakury, "Dynamic analysis of a concrete chimney considering the aerodynamic damping," *Rev. IBRACON Estrut. Mater.*, vol. 12, no. 2, pp. 308–328, 2019., <http://dx.doi.org/10.1590/s1983-41952019000200006>.
- [13] J. C. Mota, "Study of non-deterministic dynamic structural behavior and evaluation of human comfort in tall buildings," Ph.D. dissertation, Civ. Eng. Postgrad. Program., State Univ. Rio de Janeiro, Rio de Janeiro, 2023.
- [14] Associação Brasileira de Normas Técnicas, *Projeto de Estruturas de Concreto – Procedimento*, ABNT NBR 6118, 2014.
- [15] M. T. Asyikin, "CFD simulation of vortex induced vibration of a cylindrical structure," Ph.D. dissertation, Inst. Bygg, Anlegg Trans., Trondheim, Norway, 2012.
- [16] D. C. Wilcox et al., *Turbulence Modeling for CFD*. La Canada, CA, USA: DCW Ind., 2006.
- [17] B. E. Launder and D. B. Spalding, "The numerical computation of turbulent flows," *Comput. Methods Appl. Mech. Eng.*, vol. 3, no. 2, pp. 269–289, 1974, [http://dx.doi.org/10.1016/0045-7825\(74\)90029-2](http://dx.doi.org/10.1016/0045-7825(74)90029-2).
- [18] P. V. Nielsen, "Computational fluid dynamics and room air movement," *Indoor Air*, vol. 14, no. s7, pp. 134–143, 2004, <http://dx.doi.org/10.1111/j.1600-0668.2004.00282.x>.
- [19] Y. Tominaga and T. Stathopoulos, "Numerical simulation of dispersion around an isolated cubic building: comparison of various types of k-ε models," *Atmos. Environ.*, vol. 43, no. 20, pp. 3200–3210, 2009, <http://dx.doi.org/10.1016/j.atmosenv.2009.03.038>.
- [20] V. Yakhot, S. A. Orszag, S. Thangam, T. B. Gatski, and C. G. Speziale, "Development of turbulence models for shear flows by a double expansion technique," *Phys. Fluids A Fluid Dyn.*, vol. 4, no. 7, pp. 1510–1520, 1992, <http://dx.doi.org/10.1063/1.858424>.
- [21] R. S. Eger, "Modeling turbulent flows under the action of alternating rotation," M.S. thesis, Fed. Univ. Santa Catarina, Florianópolis, 2010.
- [22] W. Jones and B. Launder, "The prediction of laminarization with a two-equation model of turbulence," *Int. J. Heat Mass Transf.*, vol. 15, no. 2, pp. 301–314, 1972, [http://dx.doi.org/10.1016/0017-9310\(72\)90076-2](http://dx.doi.org/10.1016/0017-9310(72)90076-2).

- [23] P. J. Richards and R. P. Hoxey, "Appropriate boundary conditions for computational wind engineering models using the k- $\epsilon$  turbulence model," *J. Wind Eng. Ind. Aerodyn.*, vol. 46-47, pp. 145–153, 1993, [http://dx.doi.org/10.1016/0167-6105\(93\)90124-7](http://dx.doi.org/10.1016/0167-6105(93)90124-7).
- [24] B. Blocken, "Computational fluid dynamics for urban physics: importance, scales, possibilities, limitations and ten tips and tricks towards accurate and reliable simulations," *Build. Environ.*, vol. 91, pp. 219–245, 2015, <http://dx.doi.org/10.1016/j.buildenv.2015.02.015>.
- [25] J. Revuz, D. M. Hargreaves, and J. S. Owen, "On the domain size for the steady-state CFD modelling of a tall building," *Wind Struct.*, vol. 15, no. 4, pp. 313–329, 2012, <http://dx.doi.org/10.12989/was.2012.15.4.313>.
- [26] M. Belloli, L. Rosa, and A. Zasso, "Wind loads and vortex shedding analysis on the effects of the porosity on a high slender tower," *J. Wind Eng. Ind. Aerodyn.*, vol. 126, pp. 75–86, 2014, <http://dx.doi.org/10.1016/j.jweia.2014.01.004>.
- [27] L. Caracoglia, "A stochastic model for examining along-wind loading uncertainty and intervention costs due to wind-induced damage on tall buildings," *Eng. Struct.*, vol. 78, pp. 121–132, 2014, <http://dx.doi.org/10.1016/j.engstruct.2014.07.023>.
- [28] M. Shinozuka and C. M. Jan, "Digital simulation of random processes and its applications," *J. Sound Vibrat.*, vol. 25, no. 1, pp. 111–128, 1972, [http://dx.doi.org/10.1016/0022-460X\(72\)90600-1](http://dx.doi.org/10.1016/0022-460X(72)90600-1).
- [29] N. Isyumov, "Criteria for acceptable wind-induced motions of tall buildings", in *Proc. Int. Conf. Tall Build Counc. Tall Build Urban Habitat*, Rio de Janeiro, 1993.
- [30] A. Kareem, T. Kijewski, and Y. Tamura, "Mitigation of motions of tall buildings with specific examples of recent applications," *Wind Struct.*, vol. 2, no. 3, pp. 201–251, 1999, <http://dx.doi.org/10.12989/was.1999.2.3.201>.
- [31] A. Kareem, "Wind-induced response of buildings: a serviceability viewpoint", in *Proc. Nat. Eng. Conf.*, Miami Beach, FL.
- [32] Architectural Institute of Japan, *Guidelines for the Evaluation of Habitability to Building Vibration*. Tokyo: AIJ, 1991.
- [33] N. H. Melbourne and T. R. Palmer, "Accelerations and comfort criteria for buildings undergoing complex motions," *J. Wind Eng. Ind. Aerodyn.*, vol. 41, no. 1-3, pp. 105–116, 1992, [http://dx.doi.org/10.1016/0167-6105\(92\)90398-T](http://dx.doi.org/10.1016/0167-6105(92)90398-T).
- [34] J. W. Reed, *Wind Induced Motion and Human Discomfort in Tall Buildings* (Research Report 71-42). Massachusetts: Massachusetts Inst. Technol., 1971.
- [35] A. Irwin, "Motion in tall buildings", in *Proc. Conf. Tall Build, 2nd Century of the Sky-scraper*, Chicago, USA, 1981.
- [36] International Organization for Standardization, *Guidelines for the evaluation of response of occupants of fixed structures, especially buildings and off-shore structures to low-frequency horizontal motion (0.063 to 1 Hz)*, ISO 6897-1984(E), Geneva, 1984.
- [37] T. Goto, "Studies on wind-induced motion of tall buildings based on occupants reactions," *J. Wind Eng. Ind. Aerodyn.*, vol. 13, no. 1-3, pp. 241–252, 1983, [http://dx.doi.org/10.1016/0167-6105\(83\)90145-9](http://dx.doi.org/10.1016/0167-6105(83)90145-9).
- [38] H. Bachmann et al., *Vibration problems in structures - Practical guidelines*. Basel, Switzerland: Institut für Baustatik und Konstruktion, Birkhäuser, 1995.

---

**Author contributions:** LFM: conceptualization, formal analysis, methodology, writing; JGSS: conceptualization, supervision, formal analysis, methodology, writing.

**Editors:** Mauro Real, Guilherme Aris Parsekian.